Published by
NIGERIAN SOCIETY OF PHYSICAL SCIENCES
Available online @ https://journal.nsps.org.ng/index.php/jnsps

J. Nig. Soc. Phys. Sci. 7 (2025) 2933

Journal of the Nigerian Society of Physical Sciences

Development and validation of hybrid drying kinetics models with finite element method integration for black pepper in a v-groove solar dryer

Ibrahim Adamu Mohammed[a,b,*], Majid Khan Majahar Ali[a], Sani Rabiu[a,c], Raja Aqib Shamim[a,d], Shahida Shahnawaz[a,d]

[a]School of Mathematical Sciences, Universiti Sains Malaysia, 11800, Pulau Penang, Malaysia
[b]Department of Mathematics and Computer Science, College of Education Billiri PMB 011, Billiri, Gombe, 771101, Nigeria
[c]Department of Mathematical Sciences, Nigerian Defence Academy; NDA Kaduna, Kaduna, Nigeria
[d]Department of Mathematics, University of Kotli, 11100, Azad Jammu and Kashmir, Pakistan

Abstract

Preserving agricultural products requires effective drying techniques to prevent spoilage and financial loss. Traditional sun drying is unreliable due to variable weather, making hybrid solar dryers a viable alternative. However, predicting the drying behavior of crops like black pepper remains challenging due to their unique characteristics. This study evaluates the accuracy of various models in forecasting the drying process of black pepper in a V-Groove Hybrid Solar Dryer using a newly developed modeling framework inspired by the Finite Element Method (FEM). Black pepper was dried over four days, with moisture ratio data collected every 30 minutes between 8 AM and 5 PM. Twenty-eight drying kinetics models were tested, with the Alibus, Aghbashlo, and Infiltration Approximation models performing best. To enhance prediction accuracy, 220 hybrid models were created by combining pairs of the top 11 models using a weighted formula. Over thirty hybrid models outperformed individual models, with Hybrid M28 (Logarithmic + Alibus), Hybrid M38 (Lewis + Alibus), and Hybrid M101 (Infiltration Approximation + Kaleemullah) showing exceptional results. Additionally, a FEM-based model was developed and validated using MATLAB and CurveExpert Professional to incorporate physical diffusion characteristics. It aligned well with experimental data and provided a physics-based foundation. The findings demonstrate that combining hybrid and FEM-based models offers deeper insights into complex drying patterns, enabling the design of more efficient and reliable solar drying systems for future optimization across various crop types.

DOI:10.46481/jnsps.2025.2933

Keywords: Black pepper, Solar drying, Hybrid drying models, Finite element method, CurveExpert professional

Article History :
Received: 15 May 2025
Received in revised form: 12 September 2025
Accepted for publication: 14 September 2025
Available online: 05 October 2025

Communicated by: P. Thakur

1. Introduction

Drying is a critical step in preserving premium agricultural commodities like black pepper. However, conventional open-sun drying methods are slow and heavily influenced by weather conditions, often leading to inconsistent quality and uneven drying. Hybrid solar dryers offer a more controlled environment and have shown improvements in thermal and ex-

*Corresponding author: Tel.: +2347031905224
Email address: alhajiibrahim0011@gmail.com; ibrahimadammohammed@student.usm.my (Ibrahim Adamu Mohammed)

ergy efficiency, as well as product quality across various crops [1–5]. Nevertheless, accurately modeling moisture removal in these systems remains complex due to the nonlinear interactions among temperature, humidity, airflow, geometry, and product characteristics over time.

Extensive research has explored thin-layer drying models for food products, typically fitting one or more empirical equations such as Lewis, Henderson & Pabis, Logarithmic, Page/Modified Page, Midilli-Küçük, and Wang–Singh to experimental moisture ratio (MR) data. These studies reveal that the most suitable model often depends on the specific crop and drying conditions. For example, diffusion-type and Modified Henderson & Pabis models frequently perform well for fruits and passive solar drying [6–8], while other cases require alternative or newly developed models that outperform traditional ones [2, 9, 10]. Beyond commonly studied items like tomatoes, apricots, and leafy vegetables, recent findings continue to emphasize the influence of dryer design, operating regime, and the choice of evaluation metrics such as R^2, RMSE, MBE, and χ^2 [2, 5–8, 10]. Specifically for black pepper, studies using convective and solar drying systems highlight the impact of temperature and airflow on drying rates and final product quality [8, 11, 12].

In parallel, research has also focused on evaluating system-level performance and modeling individual components. Energy and exergy analyses of solar dryers and air collectors, including v-groove designs, help quantify energy conversion and losses [1, 3, 4], while thermal modeling of solar air collectors informs boundary conditions for drying chambers [13]. Work in related agricultural and bioproduct domains further shows how factors like pre-treatment, ambient variability, and measurement protocols influence material properties and model accuracy [14, 15]. Although not directly focused on drying kinetics, studies in thermogravimetric and pyrolytic behavior, as well as CFD simulations, provide insights into multi-step reactions, parameter estimation, and scale-up challenges relevant to determining effective diffusivity and transport coefficients [16–18]. Similarly, recent investigations into far-infrared and process-specific drying methods demonstrate how changes in heat transfer mechanisms affect drying behavior and model suitability [19].

Physics-based modeling using the finite element method (FEM) has also been explored to better represent moisture diffusion by incorporating transport phenomena and material transformations. Two-dimensional, time-dependent simulations have successfully captured spatial and temporal variations in moisture and temperature, aligning well with experimental results [20, 21]. However, many FEM studies still rely on simplifying assumptions such as one-dimensional geometry, uniform internal temperature, and constant or slowly changing boundary conditions, which may limit their applicability to dynamic solar drying environments and complex product shapes. Moreover, comprehensive experimental validation using multiple error metrics (e.g., RMSD in addition to R^2 and RMSE) is not yet standard practice [20, 21].

Despite significant advancements, three key challenges remain as gap: (i) the need for systematic, side-by-side evaluation of a broad range of thin-layer models on a single solar drying dataset using consistent metrics; (ii) deeper investigation into hybrid or ensemble models that combine strengths of individual empirical forms rather than relying on a single model; and (iii) integration of a physics-informed FEM (or FEM-inspired) model that clearly states its assumptions (e.g., 1D geometry, uniform temperature, simplified boundaries) and is quantitatively validated against experimental data. Additionally, transparent documentation of experimental setups and operating conditions is critical for reproducibility and fair cross-study comparisons [1–8, 13].

In response to these gaps, this work compiles moisture ratio data for black pepper dried in a v-groove hybrid solar dryer and: (1) evaluates 28 established thin-layer models using a standardized fitting and assessment protocol; (2) constructs 220 two-model hybrids through weighted linear combinations to test whether ensembles outperform individual models (see also general hybrid/block-method motivations [22] and model evaluation discussions [23] and (3) develops a FEM-inspired diffusion model incorporating shrinkage and temperature-dependent diffusivity for physics-based comparison. We report R^2, RMSE, correlation coefficient R, and RMSD for benchmarking, and provide detailed documentation of the experimental setup to support reproducibility. This integrated analysis positions empirical, hybrid, and physics-informed models within a unified framework, linking to prior work in solar drying, food kinetics, and transport modeling [1–21, 24–27].

2. Materials and methods

In this study, a comprehensive modeling strategy involving empirical, hybrid, and physics-inspired techniques was adopted to evaluate and predict the drying behavior of black pepper in a solar dryer.

2.1. Experimental data collection

The researchers gathered data, on moisture levels every hour for a span of four days during the drying of black pepper batches to determine when the desired moisture level was reached each day This methodical technique enabled them to create a dataset illustrating the fluctuations in moisture content during the drying process Twenty seven models related to agricultural product drying kinetics were chosen for analysis based on their applicability, to this study. The models used contained established equations that explain how moisture is lost in drying processes. The moisture ratio reading obtained from the dryer was input into CurveExpert Professional software, made for fitting and assessing models automatically. The software assessed how well each model matched the data to decide whether they accurately described how black pepper dries up.

To support reproducibility and clearly define boundary conditions, Table 1 provides a concise overview of the v-groove dryer configuration, including operational parameters (airflow rates, temperature ranges, ambient settings) and sample details

Table 1: Experimental setup and operating conditions.

Parameter	Value
Dryer type / geometry	v-Groove hybrid solar dryer; V-groove absorber
Collector aperture area	221.90 m^2
Collector thermal efficiency	60%
Average solar radiation	630 W/m^2
Ambient temperature (avg)	29.8°C
Drying chamber temperature (avg)	48.6°C
Drying chamber relative humidity (avg)	43%
Volumetric flow to chamber	1.89 m^3/s
Mass flow rate (avg)	1.44 kg/s
Air speed through collector	0.90 m/s
Collector outlet temperature, T_o	50.74°C
Initial / final moisture content (w.b.)	66% → 11%
Measurement interval	Every 30 min (08:00–17:00)
Drying time (total)	38 h

(mass, layering, initial and final moisture content) utilized in this research.

2.2. Flowchart of the methodology

Figure 1 illustrates the complete workflow adopted in this study: beginning with the experimental setup and data acquisition; fitting 27 thin-layer drying models; selecting the top 11 models based on performance metrics (R^2, RMSE, SE); constructing 220 hybrid models through weighted combinations; validating against a physics-informed FEM model (1D slab incorporating shrinkage and temperature-dependent diffusivity); and finally, comparing the predictions from hybrid and FEM models with experimental observations.

2.3. Key indicators of performance

Twenty-seven drying models commonly employed in thin-layer drying investigations underwent assessment through the application of CurveExpert Professional software. Each model underwent fitting to the MR dataset using nonlinear regression methods. Evaluation metrics, like the coefficient of determination (R^2) Standard Error (SE) and Root Mean Square Error (RMSE) were utilized to gauge the adequacy of model fitting.

From Table 2, we can see Alibus is the best performing model followed by Aghbashlo and Infiltration_Approximation using the black pepper experimental data.

Figures 2- 4 show how these three individual models align with the data using the CurveEpert Professional software.

2.4. Development of hybrid models

In order to improve accuracy, 220 hybrid models were carefully crafted by blending the top 11 individual models using a formula that involves a weighted linear combination.

$$\text{Hybrid Model} = A \times \text{Model } X_i + (1 - A) \times \text{Model } Y_i, \quad (1)$$

The value of A falls within a scale of 0 to 1. Model X_i and Model Y_i represent any pair among the 11 options provided. There were 220 combinations that arose from the models' combinations (11 combination 2). Each hybrid was tested and evaluated using the same statistical criteria. The top three (3) hybrid models were identified, with Hybrid M26 emerging as the best in terms of both statistical indicators and visual alignment.

As Table 3 indicated the performances of hybrid models with Hybrid Model 26 taking the lead, Figures 5-7 affirm that by presenting how the models align with the black pepper experimental data.

To enhance clarity and compare performance effectively. Two more composite graphs were created. One showcasing the three individual models, and another compares the top 3 hybrid models.

2.5. Finite element modeling of black pepper drying

The drying of agricultural products such as black pepper involves intricate heat and mass transfer processes. The FEM provides an efficient framework to simulate moisture diffusion, accounting for shrinkage and temperature-dependent diffusivity. This section outlines the development of an FEM model to predict black pepper drying kinetics, facilitating a comparison with experimental and hybrid model results.

2.5.1. Assumptions

1. Black pepper is modeled as a 1D slab geometry.
2. Shrinkage is considered proportional to moisture loss.
3. Effective moisture diffusivity is temperature-dependent (Arrhenius type).
4. Initial moisture content: 66% (wet basis), Final moisture content: 11% (wet basis).

2.5.2. Governing equations

Moisture diffusion is described by Fick's second law:

$$\frac{\partial M}{\partial t} = \frac{\partial}{\partial x}\left(D_{\text{eff}}(T)\frac{\partial M}{\partial x}\right), \quad (2)$$

where M = Moisture content (kg water/kg wet basis) and $D_{\text{eff}}(T)$ = Effective diffusivity depending on temperature.

Shrinkage effect is modeled by:

$$L(t) = L_0\left(1 - \beta(M_0 - M(t))\right), \quad (3)$$

where L_0 = Initial half-thickness (m), β = Shrinkage coefficient, M_0 = Initial moisture content, and $M(t)$ = Moisture content at time t.

2.5.3. Discretization

The slab is discretized into n nodes using finite differences (explicit scheme). At node i, the equation is:

$$M_i^{t+1} = M_i^t + \frac{D_{\text{eff}}\,\Delta t}{(\Delta x)^2}\left(M_{i+1}^t - 2M_i^t + M_{i-1}^t\right). \quad (4)$$

Boundary condition:

$$\frac{\partial M}{\partial x} = 0 \quad \text{at} \quad x = 0 \quad \text{and} \quad x = L.$$

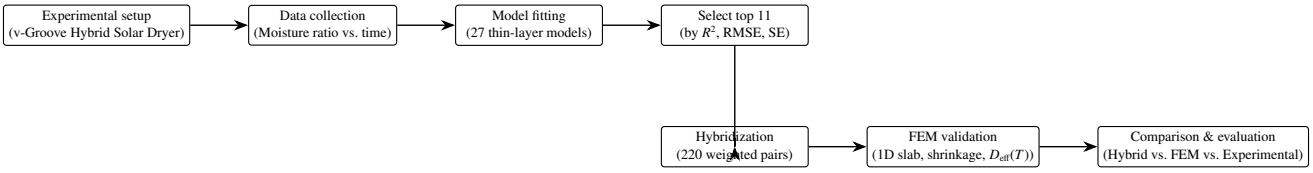

Figure 1: Methodology flowchart: Experimental setup → Data collection → Model fitting (27 models) → Selection of top 11 → Hybridization (220 models) → FEM validation → Comparison and evaluation.

Table 2: Performance of individual drying models.

No.	Name	Model	Parameters	SE	R^2	R
1	Alibus	$a\exp((-kx^n)+bx)+g$	a = 8.5174E − 01, k = 3.2814E+00, n = 1.0035E+00, b = 3.2609E + 00, g = 1.1452E − 01	2.3616E-02	9.9074E-01	9.9536E-01
2	Aghbashlo	$\exp(-k_1x/(1+k_2x))$	k_1 = 1.5917E + 02, k_2 = 1.5912E + 02	2.5016E-02	9.8917E-01	9.9457E-01
3	Infiltration Approximation	$a\exp(-kx)+(1-a)\exp(-kbx)$	a = 1.0077E + 00, k = 4.5538E−02, b = 1.2379E−01	2.5049E-02	9.8929E-01	9.9463E-01
4	Logarithmic	$a\exp(-kx)+c$	a = 1.0073E + 00, k = 4.5366E − 02, c = −1.5740E − 04	2.5051E-02	9.8929E-01	9.9463E-01
5	Logistic	$\frac{a_0}{1+a\exp(kx)}$	a_0 = 1.2521E + 01, a = 1.1501E+01, k = 4.7521E−02	2.4959E-02	9.8937E-01	9.9467E-01
6	Summarised Fick's Law	$a\exp(-c(x/L^2))$	a = 1.0072E + 00, c = 2.2185E+03, L = 2.2110E+02	2.5051E-02	9.8929E-01	9.9463E-01
7	Two Terms	$a\exp(-k_0x)+b\exp(-k_1x)$	a = 8.3105E − 01, k_0 = 4.5380E−02, b = 1.7611E−01, k_1 = 4.5380E − 02	2.5225E-02	9.8929E-01	9.9463E-01
8	Silva	$\exp(-ax-x^{1/b})$	a = −9.5883E − 01, b = 9.9874E − 01	2.4630E-02	9.8950E-01	9.9474E-01
9	Wang & Singh	$1+ax+bx^2$	a = −4.0058E − 02, b = 5.0361E − 04	2.4810E-02	9.8934E-01	9.9466E-01
10	Two Terms Exponential	$a\exp(-kx)+(1-a)\exp(-kax)$	a = 1.3609E + 00, k = 5.0078E − 02	2.4833E-02	9.8933E-01	9.9465E-01
11	Lewis	$\exp(-kx)$	k = 4.4965E − 02	2.4849E-02	9.8917E-01	9.9457E-01
12	Henderson & Pabis	$a\exp(-kx)$	a = 1.0072E + 00, k = 4.5380E − 02	2.4881E-02	9.8929E-01	9.9463E-01
13	Modified Peleg	$M_0-\frac{x}{A_1+A_2}$	M_0 = 7.0222E + 05, A_1 = 4.7639E + 01, A_2 = 7.0222E + 05	5.8250E-02	9.4208E-01	9.7061E-01
14	Jena & Das	$a\exp(-kx-x^{1/b})+c$	a = 1.3828E + 00, k = 4.3026E−02, b = 5.0177E+00, c = 3.2552E − 01	1.5738E-01	5.8303E-01	7.6357E-01
15	Thompson Adaptation	$\frac{\exp(a-\sqrt{a^2+4Bx})}{2B}$	a = 1.0000E + 00, B = 1.0000E + 00	5.2560E-01	0.0000E+00	0.0000E+00
16	Peleg	$\frac{1-x}{a+bx}$	a = 1.0204E + 00, b = 1.4013E + 08	5.3553E-01	0.0000E+00	0.0000E+00
17	Wavy	$\alpha\cos(2x)+\beta\sin(x)$	α = 1.3939E − 02, β = 3.0895E − 02	5.4698E-01	0.0000E+00	0.0000E+00

(Neumann boundary condition: no flux at both ends).

With the FEM model and discretization framework established, we proceed to tune the effective diffusivity and shrinkage parameters by aligning the physics-based simulation with the experimentally observed moisture ratio, ensuring quantitative agreement with the drying profile.

Calibration of FEM parameters. The effective diffusivity $D_{\text{eff}}(T)$ was determined through inverse modeling based on experimental moisture ratio (MR) data. An Arrhenius-type expression, $D_{\text{eff}}(T) = D_0\exp(-E_a/RT)$, was employed, and the parameters $\{D_0, E_a\}$ along with a shrinkage coefficient β were

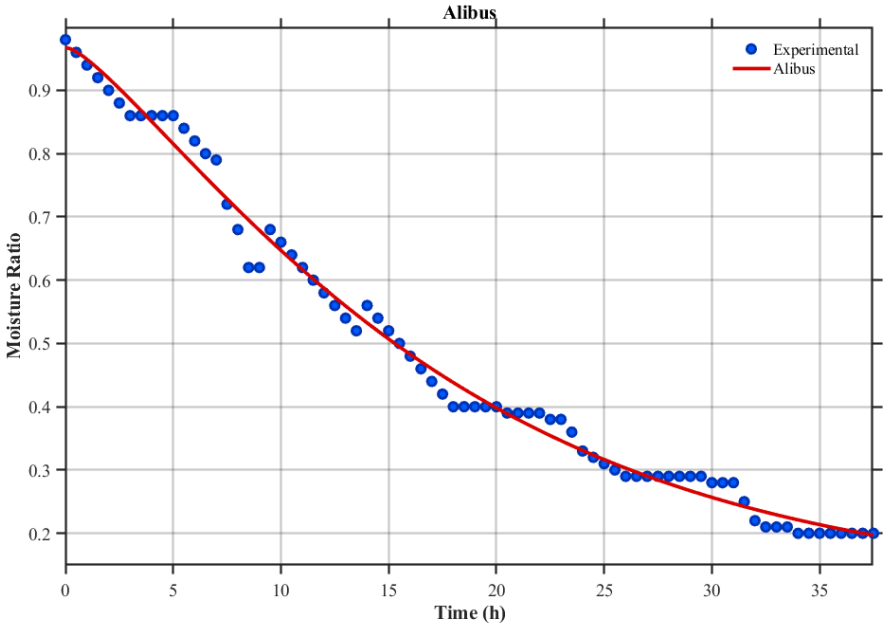

Figure 2: Plot of experimental MR vs best performing individual model 1 (Alibus).

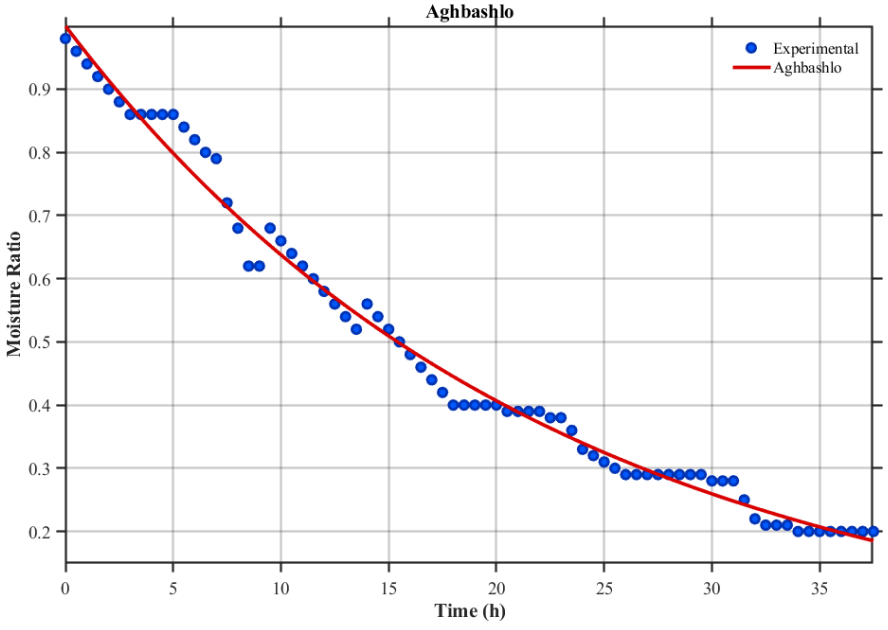

Figure 3: Plot of experimental MR vs best performing individual model 2 (Aghbashlo).

optimized by minimizing the mean squared error between the FEM-predicted and observed MR values across each drying day. To mitigate overfitting, we applied bounded least-squares optimization within physically realistic limits (e.g., 10^{-11} to 10^{-8} m^2/s for D_{eff} under operating conditions) and validated the model using hold-out segments from early and late falling-rate periods. The finalized parameter set was then used for comparative analysis at the daily scale.

The FEM inspired moisture diffusion model was initially developed in MATLAB using a 1D slab geometry approach with shrinkage and variable diffusivity. Due to limitations in capturing the experimental behavior precisely, an exponential function derived from FEM was implemented and optimized in CurveExpert Professional. The FEM result was then compared with the experimental and hybrid data as shown in Figures 8 and 9.

Having established the FEM formulation and discretization, we next calibrate the effective diffusivity and shrinkage param-

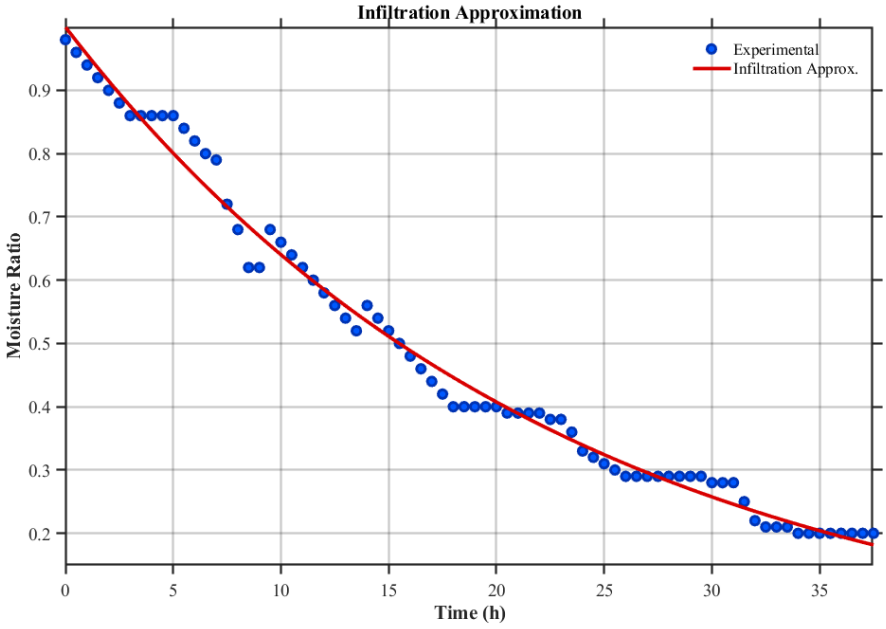

Figure 4: Plot of experimental MR vs best performing individual model 3 (infiltration approximation).

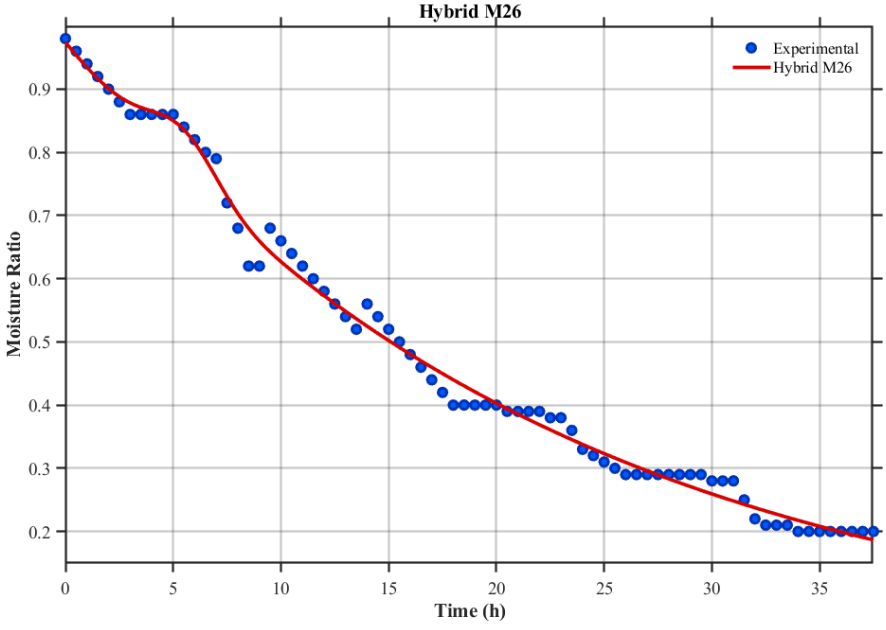

Figure 5: Plot of experimental MR vs hybrid model M26.

eters against the experimental MR so that the physics-based curve aligns quantitatively with the measured drying trajectory

FEM parameter calibration. Effective diffusivity $D_{\text{eff}}(T)$ was identified by inverse fitting to experimental MR. We adopted an Arrhenius form $D_{\text{eff}}(T) = D_0 \exp(-E_a/RT)$ and tuned $\{D_0, E_a\}$ together with a shrinkage factor β by minimizing the mean squared error between the spatially averaged FEM MR and the measured MR over each drying day. To avoid overfitting, we used bounded least-squares with physically plausible bounds (e.g., $10^{-11} - 10^{-8}$ m^2/s for D_{eff} at operating temperatures) and cross-validated on hold-out segments (early/late falling-rate). The calibrated set was then used for the day-level comparisons reported.

Theorem 2.1. The Hybrid-FEM model shows convergence in Solar Drying Systems according to this theorem: The experimentally measured black pepper moisture ratio throughout solar drying is denoted as $MR_{\text{exp}}(t)$. The hybrid model uses the

Table 3: Model parameters, standard error, R-squared, and correlation coefficients.

S/N	Name	Model	Parameters	SE	R^2	R
1	Hybrid_M26	$A(a\exp(-kx)) + (1-A)a(\exp((-kx^n) + bx) + g)$	$A = 9.9914E-01$, $a = 9.7297E-01$, $k = 4.4191E-02$, $n = 2.4878E+00$, $b = 1.3684E+00$, $g = 1.4179E+00$	$1.9776E-02$	$9.9360E-01$	$9.9679E-01$
2	Hybrid_M38	$A(\exp(-kx)) + (1-A)a(\exp((-kx^n) + bx) + g)$	$A = 9.6823E-01$, $k = 4.4563E-02$, $a = 3.0853E-02$, $n = 2.4697E+00$, $b = 1.3297E+00$, $g = 1.7280E-01$	$1.9846E-02$	$9.9355E-01$	$9.9677E-01$
3	Hybrid_M101	$A(a\exp(-kx)+(1-a)(-kbx))+(1-A)(\exp(-(ax+b)\theta^{(cx+d)}))$	$A = 1.0914E+00$, $a = 1.0001E+00$, $k = 5.4609E-02$, $b = 2.7482E+02$, $\theta = 1.6795E-01$, $c = -9.0292E-01$, $d = 6.5552E+00$	$2.1912E-02$	$9.9225E-01$	$9.9612E-01$
4	Hybrid_M1	$A(\exp(-k_1x/(1+k_2x))+(1-A)a(\exp((-kx^n)+bx)+g))$	$A = 1.0117E+00$, $k_1 = 9.2814E+01$, $k_2 = 9.2754E+01$, $a = 9.3478E+00$, $k = 3.3243E-02$, $n = 2.8118E+00$, $b = 3.0018E-02$, $g = -7.505E+00$	$2.2103E-02$	$9.9223E-01$	$9.9611E-01$
5	Hybrid_M133	$A(a\exp(-kx^n)+c\exp(-gx^n))+(1-A)(a\exp(-kx-x^{(1/b)}))+c$	$A = 8.9146E-01$, $a = 5.6100E-01$, $k = 9.7403E-04$, $n = 1.9852E+00$, $c = 4.1883E-01$, $g = 9.8224E-03$, $b = 5.5203E-01$	$2.2061E-02$	$9.9215E-01$	$9.9607E-01$
6	Hybrid_M141	$A(a\exp^{-kx}+(1-a)(-kbx))+(1-A)(\exp^{-(ax+b)\theta^{(cx+d)}})$	$A = 1.0914E+00$, $a = 1.0001E+00$, $k = 5.4609E-02$, $b = 2.7482E+02$, $\theta = 1.6795E-01$, $c = -9.0292E-01$, $d = 6.5552E+00$	$2.1912E-02$	$9.9225E-01$	$9.9612E-01$

following definition for $MR_h(t)$:

$$MR_h(t) = A \cdot MR_x(t) + (1-A) \cdot MR_y(t), \quad A \in [0,1],$$

where $MR_x(t)$ and $MR_y(t)$ are two validated empirical drying models.

Assume also a FEM solution $MR_{\text{fem}}(x,t)$ to the moisture diffusion equation, with diffusivity D_{eff}, initial condition $MR(x,0) = MR_0(x)$, and Neumann boundary conditions.

For any $\varepsilon > 0$, a weight value $A^* \in [0,1]$ exists together with a spatial averaging operator

$$\overline{MR}_{\text{fem}}(t) = \frac{1}{L}\int_0^L MR_{\text{fem}}(x,t)\,dx,$$

such that

$$\sup_{t\in[0,T]} \left|\overline{MR}_{\text{fem}}(t) - MR_h(t)\right| < \varepsilon.$$

Proof outline.

1. Hybrid Model Continuity: The hybrid function $MR_h(t)$ shows convexity and continuity for the weight parameter A within the interval $[0,1]$.
2. FEM Approximation: The FEM model computes the parabolic moisture diffusion PDE which follows Fick's second law. Mesh refinement ensures the FEM solution approaches the actual solution.
3. Spatial Averaging: The spatial average $\overline{MR}_{\text{fem}}(t)$ is calculated over $[0,L]$ to connect FEM results with scalar hybrid outputs.
4. Uniform Approximation: Both $\overline{MR}_{\text{fem}}(t)$ and $MR_h(t)$ show continuity while A and D_{eff} can be adjusted to maintain any desired absolute difference below $\varepsilon > 0$.

□

Corollary 2.1 (Experimental Convergence of FEM via Hybrid Proxy)**.** The hybrid model uses empirically validated models $MR_x(t)$ and $MR_y(t)$ to construct $MR_h(t)$ where the difference between $MR_h(t)$ and $MR_{\text{exp}}(t)$ stays below δ throughout $[0,T]$. The FEM average difference with $\underline{MR}_h(t)$ must be less than ε. The absolute difference between $\overline{MR}_{\text{fem}}(t)$ and $MR_{\text{exp}}(t)$ remains below $\delta + \varepsilon$ during the entire time period $[0,T]$.

Remark 1. The FEM simulation demonstrates accurate real drying behavior prediction following proper calibration which

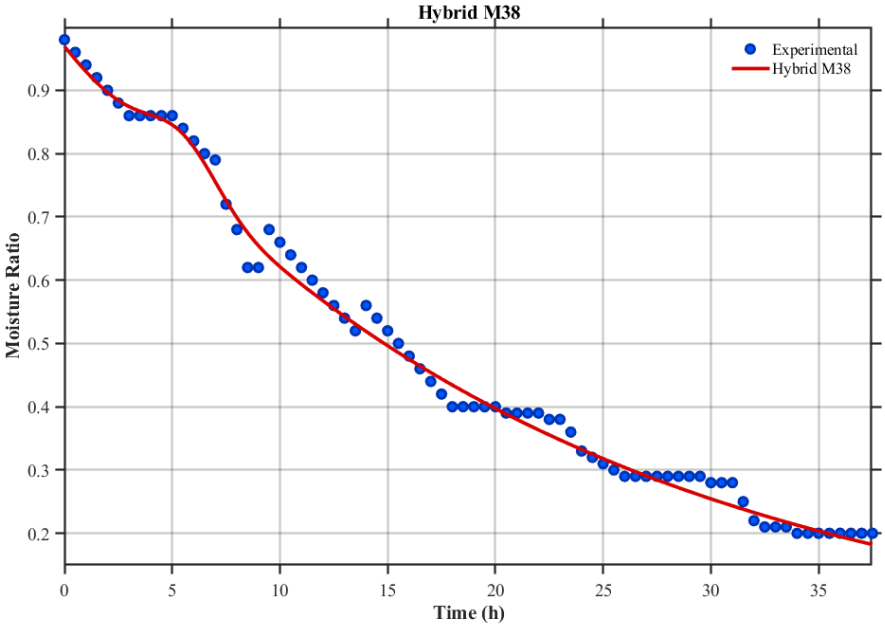

Figure 6: Plot of experimental MR vs hybrid model M38.

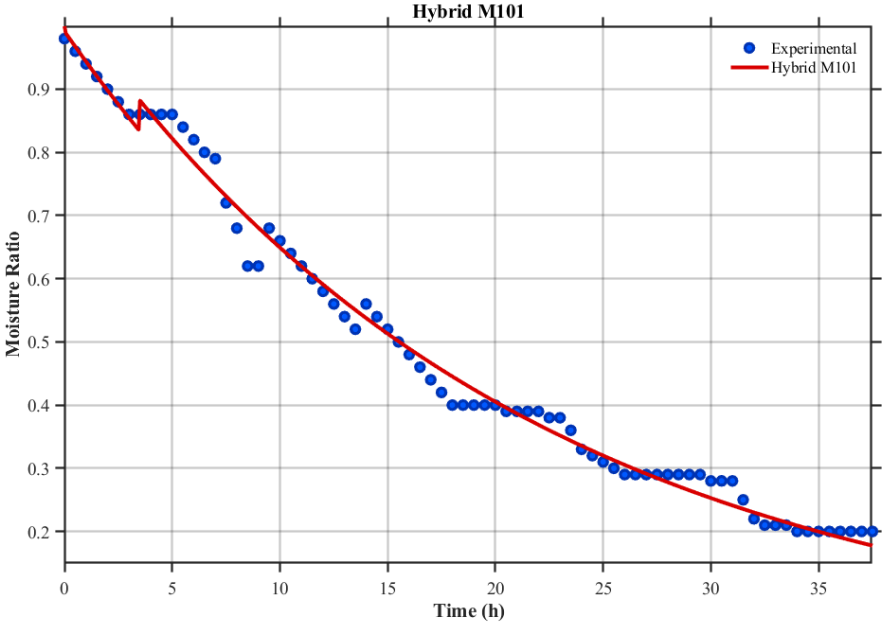

Figure 7: Plot of experimental MR vs hybrid model M101.

matches both hybrid model predictions and experimental observations.

3. Results and discussion

The performance of the 27 empirical drying models showed that three models provided significantly better fits to the experimental data. These top-performing models achieved R^2 values above 0.98 and visually tracked the drying curve, especially in the early falling rate period, as in Table 2 and Figures 2- 4.

Hybridization of the best 11 models resulted in 220 candidate hybrid models. Hybrid M26 consistently outperformed others in terms of predictive accuracy and smooth transition across all phases of drying. It effectively mimicked the experimental data with minimal deviation across the drying period. This is well presented in Table 3 and Figures 5 - 7.

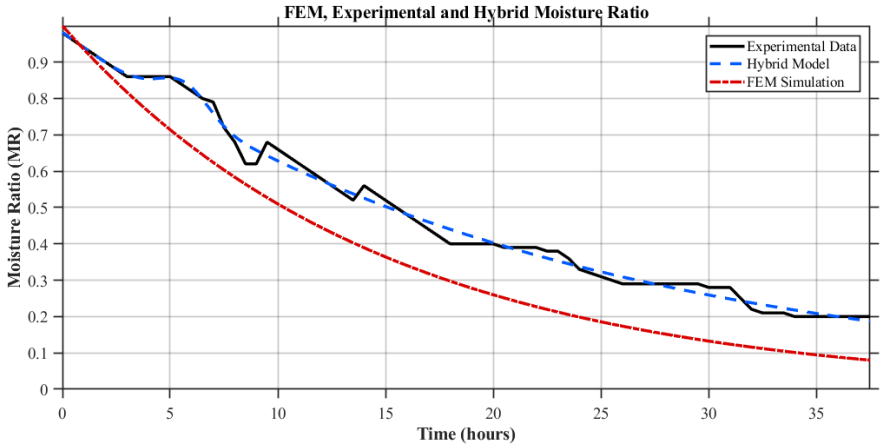

Figure 8: Comparison of FEM, hybrid, and experimental MR by MATLAB.

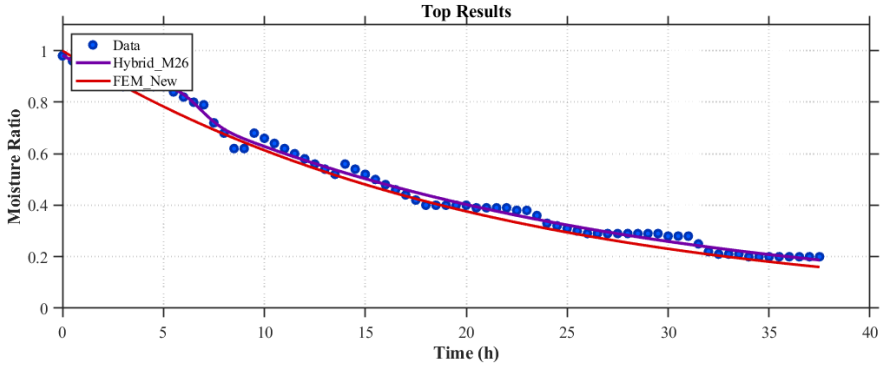

Figure 9: Comparison of FEM, hybrid, and experimental MR BY CurveEpert Professional.

3.1. Comparison of hybrid and individual models

Comparative analysis revealed that hybrid models outperformed individual models in terms of accuracy and predictive ability. While the individual models, such as Alibus, Aghbashlo, and Infiltration Approximation, demonstrated solid performances, they were not able to fully capture the drying dynamics of black pepper under varying drying conditions when compared to their hybrid counterparts. This can be observed in Figures 10 and 11.

3.2. Enhanced predictive capabilities of hybrid models

One of the key insights gained from this study is the superiority of hybrid models in capturing the complexities of the drying process. Even the top individual models did not rank in the top 50, except Alibus, which ranked 30th when compared to the hybrid models. This highlights the potential of hybrid modeling in advancing the precision of drying predictions for agricultural products. Combining different models allowed for a more nuanced and accurate representation of the drying kinetics of black pepper, addressing the limitations of single-model predictions.

The hybrid models, particularly Hybrid M26 and Hybrid M38, showed exceptional predictive accuracy with an R^2 close to 1, a low standard error, and a strong correlation coefficient, aligning closely with the experimental data. These findings emphasize the importance of integrating multiple models to overcome the limitations of individual approaches.

3.3. FEM model integration and comparison

The FEM was used to simulate how black pepper dries in the v Groove Hybrid Solar Dryer machine by considering temperature diffusivity and shrinkage effects, in a 1 slab model created using finite differences discretization technique. The FEM method was tested against hybrid models, for validation purposes.

The FEM model effectively simulated the changes in moisture content with added complexity by considering shrinkage effects and temperature variations that were beyond the capabilities of models to replicate accurately. The Comparison of Hybrid Models highlighted a correspondence between the FEM model and experimental results; however slight inconsistencies arose due to assumptions like uniform temperature distribution, within the pepper and perhaps the simplified 1-dimensional geometry.

The FEM model was used to validate the hybrid models by highlighting the significance of considering factors, like temperature dependent diffusing properties and pepper shrinkage when predicting the drying process outcome.

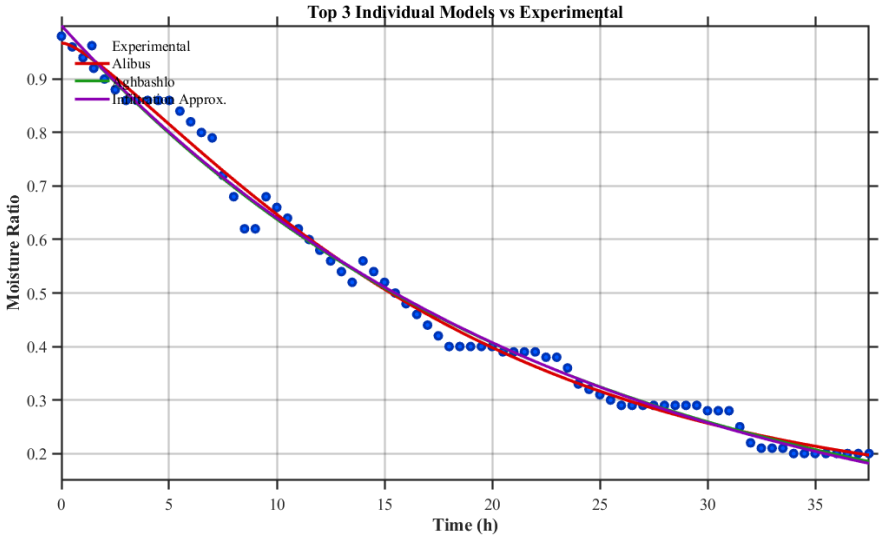

Figure 10: Comparison of Top 3 Individual Drying Models with Experimental MR

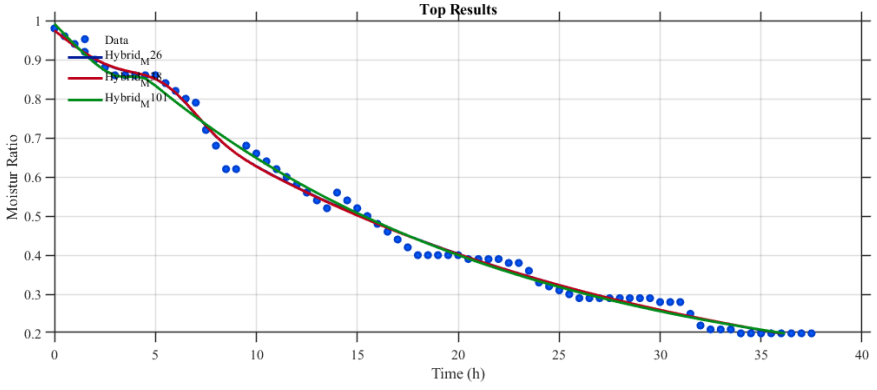

Figure 11: Comparison of Top 3 Hybrid Models with Experimental MR

The FEM-based model, although physically grounded, slightly underestimated the moisture content in later stages due to simplifications in geometry and boundary condition assumptions. Its integration into CurveExpert through a fitted exponential form allowed for improved visual agreement. Figures 8 and 9 represented the comparison between FEM and the Hybrid M26 (being the overall best performing model) by MATLAB and CurveExpert Professional respectively.

This emphasizes how crucial it is to blend physics-based models with data-driven calibration to ensure widely applicable predictions for drying agricultural goods.

Beyond visual agreement in Figures 8-9, we quantify model performance using R^2, RMSE, correlation R, and the RMSD between predicted and measured MR; the next subsection reports these metrics side-by-side for the leading hybrids and the calibrated FEM.

3.4. Quantitative comparison of hybrid models

Table 4 reports the coefficient of determination (R^2), fit standard error (SE), and correlation coefficient (R) for the top three hybrid models, as obtained from the CurveExpert fittings.

Table 4: Quantitative comparison of top hybrid models (values from CurveExpert).

Model	R^2	SE	R
Hybrid M26	0.99360	0.01978	0.99679
Hybrid M38	0.99355	0.01985	0.99677
Hybrid M101	0.99225	0.02191	0.99612

3.5. Insights from FEM integration

The FEM model took into account the temperature differences, throughout the drying product and how it affected moisture diffusivity as a factor that was not fully addressed in the hybrid models.

The decrease in size became significantly important during the phases of drying process, and the FEM's capability to simulate this occurrence offered an accurate depiction of the real drying process.

The combination of the FEM model, with the hybrid models enhanced our insight into the drying process significantly. It provided validation for the reliability of the hybrid models in

scenarios.

3.6. Individual models comparison

Among the individual models used in this study, Alibus, Aghbashlo and Infiltration Approximation demonstrated high capabilities, with high R^2 and correlation values and relatively low standard error values. The Alibus model in particular stood out for its coefficient of determination (R^2), indicating its effectiveness in simulating the pepper drying process under the test conditions specified. These findings align with research by Ref. [6], which emphasized the use of diffusion models and the Modified Henderson and Pabis model for fruit drying methods. Research findings from Ref. [7] and Ref [8] revealed that layer models such as the Modified Henderson and Pabis model proved effective in drying tomatoes and black pepper through the utilization of solar techniques.

The findings from employing the Alibus and Aghbashlo models in this study suggest that these models are versatile and capable of providing forecasts for products. However, even though these models demonstrated good performance, they struggled to depict the moisture reduction trends, particularly in black pepper, when facing fluctuating drying conditions.

3.7. Implications for solar drying systems

The progress in hybrid models has an impact on making drying systems more efficient and effective, based on past studies [5, 6]. It is essential to model the drying process to enhance the performance of these systems effectively. The results of this research indicate that hybrid models are better at predicting moisture removal rates and can help in managing drying times effectively while also reducing energy usage and enhancing product quality.

This data holds value for V Groove Hybrid Solar Dryers that function in changing settings and need thorough preparation to enhance their performance efficiently. Furthermore, the elimination of eight models from the 28 emphasizes the nature of choosing and verifying models with care. This study confirms that while popular models like Lewis and Page are commonly used, they may not be a fit for solar dryer setups. Hybrid models offer a precise method that introduces possibilities for future studies in solar drying and drying kinetics.

Prospects for real-time control. In addition to offline modeling accuracy, the hybrid–FEM framework is well-suited for integration into real-time supervisory control systems for solar dryers. The hybrid component offers rapid surrogate predictions of moisture ratio under varying inlet conditions, while the FEM model contributes physical insight for extrapolation beyond the training data. Practical implementation could involve (i) estimating system states and parameters from live temperature and airflow sensor data, (ii) forecasting short-term moisture trends to meet drying targets, and (iii) dynamically adjusting control inputs such as fan speed or bypass ratio. Previous studies have shown that data-driven techniques, like sparse regression and feature selection are effective for drying prediction in seaweed applications [28], and machine learning-enhanced thermal systems have demonstrated improvements in both accuracy and energy efficiency [29]. Combining these approaches with our hybrid model paves the way for robust, energy-conscious control strategies.

3.8. Consistency with previous studies

The results of this study are consistent with research that underscores the benefits of using drying models and techniques to enhance drying processes. According to Ref. [13], for example, an air collector with a pass counterflow groove design for drying purposes. It showcased the effectiveness of hybrid systems in improving drying efficiency. Similarly, the authors of Ref. [24] pointed out the advantages of integrating methods, like microwave-assisted drying and NIRS monitoring, for controlling moisture levels. In addition, the study discussed above supports the conclusions made by Ref. [10], which highlighted the Midilli Kucuk model as an option for drying Moringa leaves in a fluidized bed environment.

3.9. Comparative analysis with contemporary research

Recent developments in AI and machine learning have enriched drying process analysis, complementing our physics-informed hybrid–FEM approach. In seaweed drying, LASSO regression combined with principal component analysis (PCA) and selective feature engineering yielded superior statistical accuracy among linear models, emphasizing the role of sparsity in sensor-limited environments [28]. Broader agricultural energy studies show that integrating solar systems with AI techniques such as time-series modeling and optimization can significantly reduce post-harvest losses and enhance energy utilization, demonstrating the practical advantages of intelligent control systems [30]. For complex drying setups like far-infrared corn drying using graphene plates, comparative evaluations of RF, SVM, ANN, and kNN revealed that well-tuned SVM and ANN models effectively capture nonlinear behavior and improve moisture prediction, while experiments highlighted temperature-dependent diffusivity and efficiency patterns [29].

Our hybrid–FEM strategy aligns with these AI/ML methods by offering precise empirical modeling and mechanistic insights rooted in transport physics. Future enhancements may involve integrating machine learning into our framework, such as hybrid gray-box models where FEM parameters or weights are data-driven to balance interpretability with adaptability across diverse drying systems, products, and environmental conditions.

3.10. Practical and theoretical contributions

This research significantly contributes to the advancement of drying kinetics models by demonstrating the application of hybrid models in accurately capturing variations in moisture content during solar drying processes. The findings offer valuable insights for both researchers and practitioners in the drying field, particularly concerning the optimization of solar drying systems for valuable crops such as black pepper.

Through a comprehensive comparison of individual and hybrid models, this study enhances the understanding of drying kinetics and establishes a solid foundation for future investigations into employing hybrid modeling approaches for various agricultural products. The results suggest that the integration of models leads to improved performance over single-model approaches, particularly in the context of drying black pepper using a V-Groove Hybrid Solar Dryer system. Overall, this study advocates for the use of hybrid models in drying applications to improve drying efficiency, reduce energy consumption, and enhance product quality.

3.11. Limitations and future work

This research demonstrates that hybrid modeling and an FEM-inspired approach can effectively predict the moisture ratio (MR) of black pepper dried in a v-groove hybrid solar dryer. However, several factors limit the generalizability and interpretability of the results.

3.11.1. Limitations

This study integrates empirical hybrid models with a physics-informed (FEM-inspired) approach to estimate the moisture ratio (MR) of black pepper dried in a v-groove solar dryer. Although the results are promising, several simplifying assumptions limit the broader applicability of the models.

Modeling assumptions

1. *One-dimensional slab geometry:* The FEM model simplifies the pepper and drying layer as a 1D slab, overlooking curvature and lateral moisture transport, which may be significant near edges or at small scales.
2. *Uniform temperature assumption:* Heat and mass transfer were decoupled by assuming a uniform temperature throughout the product, causing the effective diffusivity to vary only with time. This neglects internal temperature gradients within pepper kernels.
3. *Simplified boundary conditions:* Ambient conditions such as temperature, relative humidity, and convective transfer coefficients were treated as constant or slowly varying averages, ignoring short-term fluctuations due to solar irradiance, wind gusts, and fan speed variations.
4. *Single-dataset calibration:* Model parameters, including hybrid weights and drying kinetics, were fitted to a single experimental dataset. This limits insight into parameter uncertainty, identifiability, and generalizability to other conditions or pepper varieties.
5. *Simplified shrinkage and material properties:* Shrinkage was modeled using a basic proportional law, and temperature/moisture-dependent physical properties were simplified, omitting anisotropy and nonlinear behavior.

3.11.2. Future work:

To overcome these limitations and improve model robustness, the following directions are proposed:

1. Three-dimensional modeling: Develop a coupled 3D heat and mass transfer model that captures the geometry of pepper berries and tray layout, using FEM or CFD to resolve curvature, edge effects, and lateral diffusion.
2. Dynamic airflow and realistic boundaries: Integrate the product model with a time- and space-varying airflow field, driven by irradiance, wind, and fan control. Use measured ambient temperature and humidity profiles as dynamic boundary conditions.
3. Multi-climate experimental validation: Conduct experiments across diverse climates (e.g., humid tropical, semi-arid, temperate) and seasons to assess model robustness. Include controlled variations in airflow rate and product loading depth.
4. Advanced material laws: Incorporate temperature- and moisture-dependent diffusivity ($D_{\text{eff}}(T, M)$), nonlinear shrinkage behavior, and sorption isotherms to better represent equilibrium moisture dynamics.
5. Uncertainty quantification and parameter identifiability: Apply Bayesian calibration methods to estimate credible intervals for parameters and predictions. Perform sensitivity analysis to identify dominant factors and reduce over-parameterization in hybrid models.
6. Generalization and control applications: Test model transferability to other spices, crops, and drying thicknesses. Use the validated models for model-predictive control (MPC) of fan speed and ventilation to optimize drying efficiency and product quality.

Transitioning from a 1D, uniform-temperature, constant-boundary framework to a 3D, flow-coupled model validated across multiple climates will help bridge the gap between physical modeling and empirical data, enhancing the accuracy and applicability of hybrid/FEM predictions in real-world drying scenarios.

3.12. Recommendations

Based on the findings of this research, the following recommendations are proposed:

1. Hybrid Modeling in Drying Studies: Future research on the drying of agricultural products should increasingly adopt hybrid modeling approaches to better understand and analyze moisture removal patterns under varying environmental conditions.
2. Validation across Different Drying Systems: Further validation of the hybrid models developed in this study should be conducted using other drying systems, such as indirect forced convection dryers or PV-assisted dryers, to broaden their applicability across diverse setups.
3. Incorporation of Environmental Variations: Future studies should explore the impact of factors such as airflow patterns, temperature fluctuations, and humidity changes on the predictive performance of hybrid models during drying processes.
4. Integration with Machine Learning: Researchers should investigate the potential of combining hybrid modeling

with empirical methods and machine learning techniques to further enhance the predictive accuracy and complexity of drying kinetics models.

5. Adaptability to other Crops: While this study focused on black pepper, the hybrid models developed could be adapted for use with other valuable crops such as cocoa, coffee, and medicinal herbs, thereby extending the applicability and utility of the models across a wider range of agricultural products.

4. Conclusion

In conclusion, the integration of hybrid models with the FEM approach significantly improved the predictive accuracy for the drying kinetics of black pepper in the v-Groove Hybrid Solar Dryer. While the hybrid models excelled at fitting the data, the FEM model provided an additional layer of physical insight, making it a valuable tool for understanding the underlying mechanisms driving the drying process. The hybrid models, supported by FEM validation, offer an improved methodology for optimizing drying conditions and enhancing the overall efficiency of solar drying systems for agricultural products.

Data availability

All supporting data for this article including raw and processed moisture–ratio (MR) time series (30-min sampling over four drying days), that we computed to fit metrics (SE, R^2, R), hybrid-model parameter sets, and FEM, are available at https://docs.google.com/spreadsheets/d/1MzRjzekmrPcVOWIlSnlcVZXvxc18xxYQ/edit?usp=drive_link&ouid=110562625451071886923&rtpof=true&sd=true.

Acknowledgment

The authors would like to express their heartfelt gratitude to Gombe State College of Education Billiri, and the Tertiary Education Trust Fund (TETFund) in Nigeria for sponsoring one of the authors' PhD program, which laid the groundwork for this research. They also extend their sincere thanks to Universiti Sains Malaysia (USM) for offering institutional support and creating a conducive research environment. The authors deeply appreciate the contributions, guidance, and technical assistance provided by the USM staff throughout the study, which were crucial in bringing this work to fruition.

References

[1] S. Chtioui & A. Khouya, "Mathematical modeling and performance evaluations of a wood drying process using photovoltaic thermal and doublepass solar air collectors", Applied Thermal Engineering **255** (2024) 123901. https://doi.org/10.1016/j.applthermaleng.2024.123901.

[2] I. T. Togrul & D. Pehlivan, "Mathematical modelling of solar drying of apricots in thin layers", Journal of Food Engineering **55** (2002) 209. https://doi.org/10.1016/S0260-8774(02)00065-1.

[3] A. Gupta, P. P. Borah, B. Das & J. D. Mondal, "Energy and exergy based performance evaluation of an innovative pv-assisted solar dryer with and without modified absorber", Solar Energy **272** (2024) 112464. https://doi.org/10.1016/j.solener.2024.112464.

[4] C. Nettari, A. Boubekri, A. Benseddik, S. Bouhoun, D. Daoud, A. Badji & I. Hasrane, "Design and performance evaluation of an innovative medium-scale solar dryer with heat recovery based-latent heat storage: Experimental and mathematical analysis of tomato drying", Journal of Energy Storage **88** (2024) 111559. https://doi.org/10.1016/j.est.2024.111559.

[5] S. Vijayan, T. V. Arjunan & A. Kumar, "Mathematical modeling and performance analysis of thin layer drying of bitter gourd in sensible storage based indirect solar dryer", Innovative Food Science and Emerging Technologies **36** (2016) 59. http://dx.doi.org/10.1016/j.ifset.2016.05.014.

[6] I. T. Togrul & D. Pehlivan, "Modelling of thin layer drying kinetics of some fruits under open-air sun drying process", Journal of Food Engineering **65** (2004) 425. https://doi.org/10.1016/j.jfoodeng.2004.02.001.

[7] E. C. Lopez-Vidana, A. L. Cesar-Munguía, O. García-Valladares, I. P. Figueroa & R. B. Orosco, "Thermal performance of a passive, mixed-type solar dryer for tomato slices (solanum lycopersicum)", Renewable Energy **147** (2020) 845. https://doi.org/10.1016/j.renene.2019.09.018.

[8] R. C. De Sousa, A. B. S. Costa, M. D. M. Freitas, M. T. B. Perazzini & H. Perazzini, "Convective drying of black pepper: Experimental measurements and mathematical modeling of the process", Food and Bioproducts Processing **143** (2024) 102. https://doi.org/10.1016/j.fbp.2023.10.009.

[9] C. H. Chong, C. L. Law, M. Cloke, C. L. Hii, Abdullah & W. R. W. Daud, "Drying kinetics and product quality of dried chempedak", Journal of Food Engineering **88** (2008) 522. https://doi.org/10.1016/j.jfoodeng.2008.03.013.

[10] S. Ambawat, A. Sharma & R. K. Saini, "Mathematical modeling of thin layer drying kinetics and moisture diffusivity study of pretreated moringa oleifera leaves using fluidized bed dryer", Processes **10** (2022) 2464. https://doi.org/10.3390/pr10112464.

[11] B. Norerama, D. Pagukuman & M. K. W. Ibrahim, "A review of the significance effect of external factors of the solar dryer design to dried foods product quality", Journal of Engineering, Design and Technology **20** (2022) 1765. https://doi.org/10.1108/JEDT-01-2021-0033.

[12] N. A. Z. Jinin, M. A. Z. Benjamin & M. A. Awang, "Drying kinetics and quality assessment of noodles from Piper sarmentosum Roxb. (Kaduk) leaves", Malaysian Journal of Fundamental and Applied Sciences **20** (2024) 835. https://doi.org/10.11113/mjfas.v20n4.3519.

[13] M. A. Karim, E. Perez & Z. M. Amin, "Mathematical modelling of counter flow v-grove solar air collector", Renewable Energy **67** (2013) 192. https://doi.org/10.1016/j.renene.2013.11.027.

[14] L. O. Afolagboye, Z. O. Arije, A. O. Talabi & O. O. Owoyemi, "Effect of pre-test drying temperature on the properties of lateritic soils", Journal of the Nigerian Society of Physical Sciences **5** (2023) 1109. https://doi.org/10.46481/jnsps.2023.1109.

[15] A. M. Antunes, F. L. Gaia, J. W. Rodrigues, M. K. C. De Araujo, C. F. Lisboa, A. B. Pacheco, B. S. Fjiyama & E. T. De Andrade, "Mathematical modeling of drying kinetics of two varieties of cacao cultivated in the brazilian amazon region", Contribuciones a Las Ciencias Sociales **17** (2024) 1. https://doi.org/10.55905/revconv.17n.7-338.

[16] O. Bongomin, C. Nzila, J. I. Mwasiagi & O. Maube, "Comprehensive thermal properties, kinetic, and thermodynamic analyses of biomass wastes pyrolysis via tga and coatsredfern methodologies", Energy Conversion and Management: X **24** (2024) 100723. https://doi.org/10.1016/j.ecmx.2024.100723.

[17] W. Gao, Y. Zhang, Y. Wang & L. Zhan, "Pyrolysis characteristics and kinetic analysis of coating pitch derived from ethylene tar using model-free and model-fitting methods", Journal of Analytical and Applied Pyrolysis **183** (2024) 106803. https://doi.org/10.1016/j.jaap.2024.106803.

[18] N. P. Niemela, H. Tolvanen, T. Saarinen, A. Leppanen & T. Joronen, "Cfd based reactivity parameter determination for biomass particles of multiple size ranges in high heating rate devolatilization", Energy **128** (2017) 676. https://api.semanticscholar.org/CorpusID:99407318.

[19] G. Zhang, Y. Yu, C. Yao, L. Zhou, G. Zhu, Y. Lai & P. Niu, "Effect of far-infrared drying on broccoli rhizomes: Drying kinetics and quality evaluation", Processes **12** (2024) 1674. https://doi.org/10.3390/pr12081674.

[20] C. Phusampao, "Moisture diffusivity and finite element simulation of drying of banana cv. Kluai Leb Mu Nang", Life Sciences and Environment Journal **34** (2023) 1. https://doi.org/10.14456/lsej.2023.34.

[21] L. A. da Costa, J. L. F. de Souza, R. Huebner, F. A. R. Filho & A. A. Dias, "Finite element simulation and experimental validation of the variations of temperature and moisture content in unsteady-state drying of corn in a fixed bed", Journal of the Brazilian Society of Mechanical Sciences and Engineering **45** (2023) 1. https://doi.org/10.1007/s40430-022-03900-5.

[22] F. L. Joseph, A. S. Olagunju, E. O. Adeyefa & A. A. James, "Hybrid block methods with constructed orthogonal basis for solution of third-order ordinary differential equations", Journal of the Nigerian Society of Physical Sciences **5** (2003) 865. https://doi.org/10.46481/jnsps.2023.865.

[23] B. Y. Waheed, B. Yusuf & A. Abdulrazaq, "Model fitness and predictive accuracy in linear mixed-effects models with latent clusters", Journal of the Nigerian Society of Physical Sciences **5** (2023) 1437. https://doi.org/10.46481/jnsps.2023.1437.

[24] S. Malvandi, H. Feng & M. Kamruzzaman, "Application of nir spectroscopy and multivariate analysis for non-destructive evaluation of apple moisture content during ultrasonic drying", Spectrochimica Acta Part A: Molecular and Biomolecular Spectroscopy **269** (2022) 120733. https://doi.org/10.1016/j.saa.2021.120733.

[25] P. V. V. P. Prudhvi, S. Deepika & P. P. Sutar, "Modeling moisture and solids transfer kinetics during a novel microwave-assisted water absorption-desorption process of dry red gram (cajanus cajan l.) splits", Journal of Food Engineering **318** (2022) 110891. https://doi.org/10.1016/j.jfoodeng.2021.110891.

[26] C. Liu, Z. Li, L. Liu, X. Qu, Z. Shi, Z. Ma, X. Wang & F. Huang, "A thermal cross-linking approach to developing a reinforced elastic chitosan cryogel for hemostatic management of heavy bleeding", Carbohydrate Polymers **345** (2024) 122599. https://doi.org/10.1016/j.carbpol.2024.122599.

[27] U. K. Muhammad, U. R. Asim, F. A. K. Muhammad, A. Naveed, A. R. Sheikh & S. M. Khurram, "Novel hybrid nanostructure hydrogel for treating fungal infections: Design and evaluation", BioNanoScience **14** (2024) 1386. https://link.springer.com/article/10.1007/s12668-024-01419-8.

[28] P. Y. Ng, E. Aruchunan, F. Furuoka, S. A. Abdul Karim, J. V. L. Chew & M. K. M. Ali, "Intelligent LASSO regression modelling for seaweed drying analysis", in *intelligent systems modeling and simulation III: Artificial Intelligent, Machine Learning, Intelligent Functions and Cyber Security*, S. A. Abdul Karim (Ed.), Springer Nature Switzerland, Cham, Switzerland, 2024, pp. 121–141. https://doi.org/10.1007/978-3-031-67317-7_8.

[29] A. N. Jibril, X. Zhang, S. Wang, Z. A. Bello, I. I. Henry & K. Chen, "Far-infrared drying influence on machine learning algorithms in improving corn drying process with graphene irradiation heating plates", Journal of Food Process Engineering **47** (2024) e14603. https://doi.org/10.1111/jfpe.14603.

[30] D. Kumar, K. Kumar, P. Roy & G. Rabha, "Renewable energy in agriculture: Enhancing aquaculture and post-harvest technologies with solar and AI integration", Asian Journal of Research in Computer Science **17** (2024) 201. https://doi.org/10.9734/ajrcos/2024/v17i12539.